ACS OMEGA

http://pubs.acs.org/journal/acsodf

Article

Molecular Hybrids Integrated with Benzimidazole and Pyrazole Structural Motifs: Design, Synthesis, Biological Evaluation, and Molecular Docking Studies

Ramar Sivaramakarthikeyan, Shunmugam Iniyaval, Vadivel Saravanan, Wei-Meng Lim, Chun-Wai Mai, and Chennan Ramalingan*

Cite This: *ACS Omega* 2020, 5, 10089−10098

Read Online

ACCESS | Metrics & More | Article Recommendations

ABSTRACT: Synthesis of a series of benzimidazole-ornamented pyrazoles, **6a**−**6j** has been obtained from arylhydrazine and aralkyl ketones via a multistep synthetic strategy. Among them, a hybrid-possessing *para*-nitrophenyl moiety connected to a pyrazole scaffold (**6a**) exerted the highest anti-inflammatory activity, which is superior to the standard, diclofenac sodium. While executing the 2,2-diphenyl-1-picrylhydrazyl radical-scavenging activity, a hybrid-possessing *para*-bromophenyl unit integrated at the pyrazole structural motif (**6i**) exhibited the highest activity among the hybrids examined. Besides, evaluation of anticancer potency of the synthesized hybrids revealed that the one containing a *para*-fluorophenyl unit tethered at the pyrazole nucleus (**6h**) showed the highest activity against both the pancreatic cancer cells (SW1990 and AsPCl) investigated. Considerable binding affinity between B-cell lymphoma and the hybrid, **6h** has been reflected while performing molecular docking studies (−8.65 kcal/mol). The outcomes of the investigation expose that these hybrids could be used as effective intermediates to construct more potent biological agents.

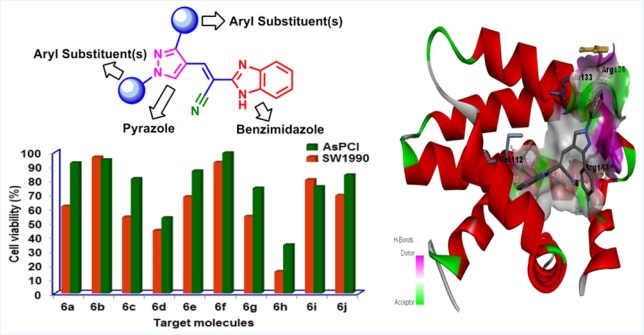

1. INTRODUCTION

Cancer has become the second leading cause of death worldwide over the past decades and is characterized by untamed augmentation and propagation of abnormal cells.[1] According to World Health Organization, nearly 9.6 million people around the world passed away because of cancer in the year 2018 and globally one in six deaths is due to cancer.[1] Particularly, because of its high invasive nature and chemo-resistance, the fatality rate as a result of pancreatic cancer is found to be reasonably higher.[2] Pancreatic cancer has the least 5 year survival rate in comparison with other cancer types due to its poor prognosis. Also, there has been no significant improvement in its survival rate since 1975. It is documented that pancreatic cancer is the fourth important origin of cancer death in the United States.[3] The typical treatment modalities, radiotherapy and chemotherapy have experienced obstruction in the hard-fought battle against cancer, with multidrug resistance being the utmost faltering block. As eradication of cancer is the extreme challenge of medicine, the present utmost need is development of novel drugs that can destroy the cancer cells.

Benzimidazole nucleus is utilized as privileged structural motif in the development of a wide range of drugs with interest in numerous therapeutic areas.[4−16] The marketed anticancer drugs tethered with benzimidazole nucleus are furnished in Figure 1.

Diverse ranges of biological potencies of agents possessing a benzimidazole unit are ascribed to the unique fused imidazole and benzene rings, which can interact with a variety of targets of biological importance in a noncovalent mode because of the presence of two hetero atoms (nitrogens) as well as its electron-rich aromatic system.[17,18] Various anticancer drugs possessing the benzimidazole structural motif are developed by researchers around the globe, and these are effectively utilized to treat cancers. Although various chemical entities possessing the benzimidazole structural motif are developed with appreciable anticancer potency, veliparib, pracinostat, bendamustine, and selumetinib are some of the drugs which are clinically used for cancers. Galeterone is yet another anticancer

Received: February 11, 2020
Accepted: April 13, 2020
Published: April 24, 2020

https://dx.doi.org/10.1021/acsomega.0c00630
ACS Omega 2020, 5, 10089−10098

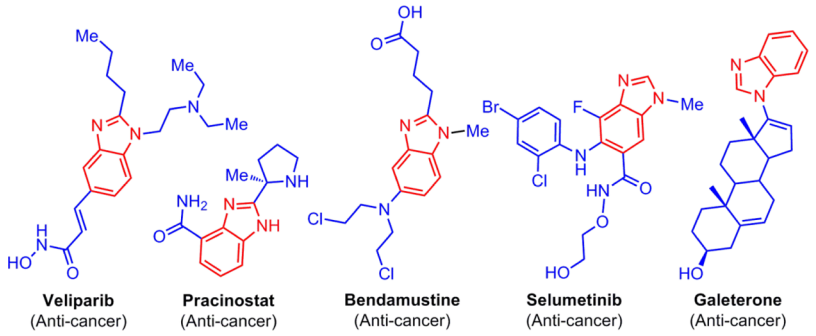

Figure 1. Anticancer drugs possessing benzimidazole structural motif.

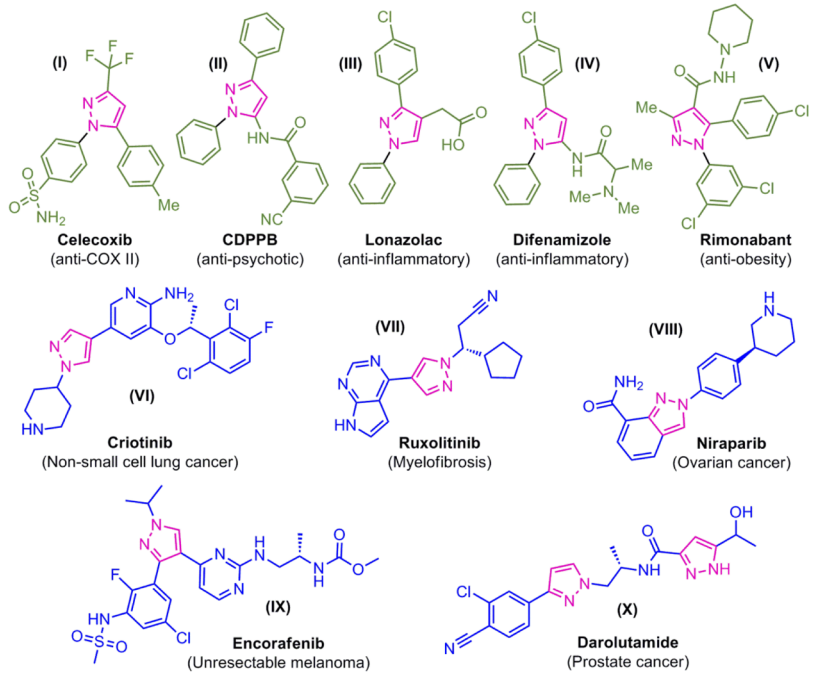

Figure 2. Anticancer drugs possessing pyrazole scaffold.

chemical entity which is under clinical trial (phase III) (Figure 1).[19−22]

On the other hand, pyrazole and its analogues are promising scaffolds in medicinal chemistry. These pyrazole molecules are one of the largely investigated groups of molecules among the family of azole. Because of the significant biological potency including anti-inflammatory, antifungal, antibacterial, antioxidant, anticancer, antidepressant, and antiviral profile of pyrazole-incorporated molecules, much attention has been focused on the same.[23−29] Representative examples of drug molecules tethered with pyrazole moiety are provided in Figure 2.[30−38]

Furthermore, a plethora of reports depicting nitrile-incorporated chemical entities and their biological importance are documented around the globe:[39−43] for example, trilostane is effectively utilized to treat breast cancer (women postmenopause). The existence of larger number of cyano pharmaceuticals is due to the biocompatibility of the nitrile.[44] Polarized triple bond, short length, and least steric requirement (cylindrical diameter of 3.6 Å) are some of the characteristics of nitriles. In addition, because of their electron richness on the nitrogen/polarizability, the nitriles play imperative role as hydrogen bond acceptors.[45]

In modern medicinal chemistry, researchers utilize the approach of pharmacophore hybridization to synthesize novel biopertinent chemical entities. This strategy is nothing but hybridization of two or more molecules possessing different bioactive structural motifs to harvest a novel bioactive chemical entity with enhanced potency.[46−52] It has been reported that molecules possessing an imidazole structural motif induce effective cell death through inhibition of PI3K-mediated PI3K/Akt/mTOR signaling pathway.[53] On the other hand, molecules containing a pyrazole scaffold induce apoptosis through caspase-dependent pathways and inactivate protein kinase B/Akt activity.[54] Provoked by the aforementioned observations and our ongoing research on synthesis of novel heterocycles as biological agents,[55−58] we designed and synthesized a series of novel chemical entities tethered with pyrazole and benzimidazole structural motifs (Figure 3) with a view to produce potent biological agents.

2. RESULTS AND DISCUSSION

2.1. Synthesis. The schematic representation for the synthesis of title benzimidazole-tethered pyrazoles, **6a−6j** is provided in Scheme 1. First, the pyrazole-based carbaldehydes, **4a−4j** are synthesized by the condensation of arylhydrazine

https://dx.doi.org/10.1021/acsomega.0c00630
ACS Omega 2020, 5, 10089−10098

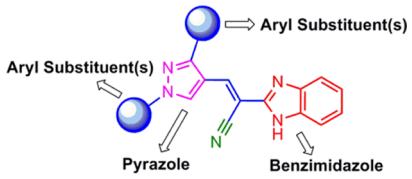

Figure 3. General structure of target molecules.

Scheme 1. Synthesis of Benzimidazole-Tethered Pyrazoles, 6a−6j

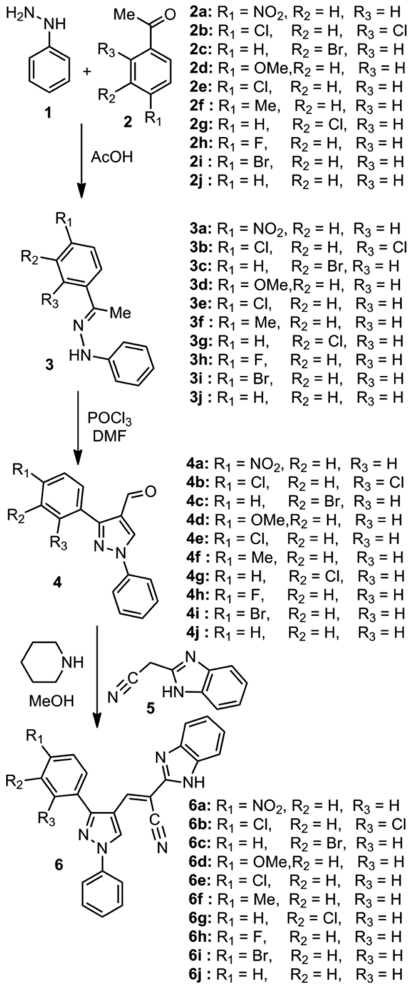

and appropriate aralkyl ketone, **2a−2j** in glacial acetic acid followed by cyclization of the hydrazone intermediates, **3a−3j** thus obtained using the Vilsmeier−Haack (VH) reaction. Knoevenagel reaction between the pyrazole-based carbaldehydes, **4a−4j** with benzimidazolyl acetonitrile, **5** in the presence of a base eventually produced the title benzimidazole-tethered pyrazoles (**6a−6j**) in good yields (Table 1).

In the IR spectra of the title chemical entities, **6a−6j**, a key band observed in the region between 3345 and 3280 cm^{-1} corresponds to N−H stretching frequency, whereas the other one observed between 2250 and 2190 cm^{-1} corresponds to CN stretching frequency. In the proton nuclear magnetic resonance (NMR) spectra of all title chemical entities, **6a−6j**, the signals for aromatic protons as well as methylenic protons resonate in the region between 9.30 and 7.15 ppm. In **6d**, a three-proton singlet results at 3.86 ppm corresponding to protons of the methoxy group integrated at one of the phenyl

Table 1. Yields and Melting Points of Target Molecules, 6a−6j

s. no.	molecules	yield (%)	MP (°C)
1	**6a**	78	336−337
2	**6b**	91	310−311
3	**6c**	87	270−271
4	**6d**	93	308−310
5	**6e**	90	258−259
6	**6f**	92	315−316
7	**6g**	88	260−261
8	**6h**	82	314−315
9	**6i**	85	298−299
10	**6j**	93	306−307

rings attached with pyrazole nucleus. Furthermore, a singlet with three protons integral resonates at 2.42 ppm in **6f** that is due to the presence of a methyl substituent on one of the phenyl moieties tethered with the pyrazole unit.

In the carbon NMR spectra of the eventual benzimidazole-tethered pyrazoles, the aromatic carbons as well as methylenic carbons resonate in the region between 161 and 115 ppm. A signal resonates at 55.7 ppm in **6d** corresponding to carbon of the methoxy group attached at one of the aryl groups. In **6f**, a signal observed at 21.3 ppm is due to carbon of the methyl group tethered at one of the aryl groups. All these key characteristics besides other bands/peaks as well as micro analysis results corroborate the formation of target molecules.

The schematic description of the reasonable mechanistic route for the construction of title chemical entities is provided in Scheme 2. The base, piperidine abstracts one of the acidic

Scheme 2. Plausible Mechanism

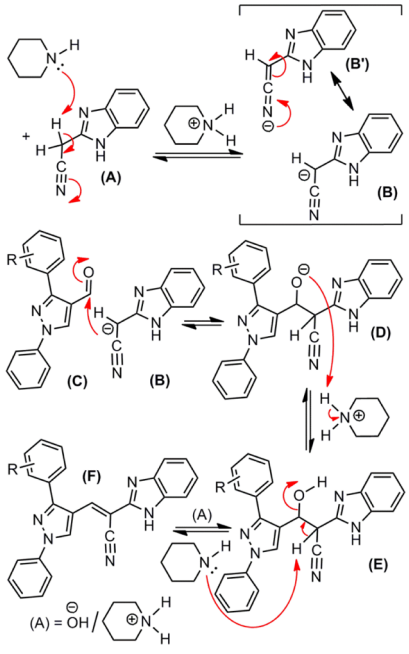

protons of the methylene group of benzimidazolyl acetonitrile, **A** to provide an anion, benzimidazolyl cyanomethanide, **B** (this can have two resonance forms, **B** and **B′**), whereas piperidine becomes piperidinium cation. The benzimidazolyl cyanomethanide **B** serves as a nucleophile, then attacks the carbonyl carbon of the pyrazole-based aldehyde, **C** to become the

https://dx.doi.org/10.1021/acsomega.0c00630
ACS Omega 2020, 5, 10089−10098

anionic intermediate, **D**. The oxide anion **D** attacks a proton of piperidinium cation and becomes hydroxyl intermediate, **E**. The hydroxyl intermediate **E** then loses a proton due to its abstraction by piperidine, followed by bond reorganization and elimination of a hydroxide ion eventually furnishes the title chemical entity (**F**).

2.2. Biological Evaluations. *2.2.1. Anti-inflammatory Activity.* The method of protein denaturation is utilized for the determination of anti-inflammatory evaluation of the target imidazole-tethered pyrazoles, **6a−6j**.[59] In this methodology, generally, the tertiary as well as secondary structure of protein would be lost when an external molecule or stress is applied. When denatured, the biological function of most biological proteins would be lost. It is well known that a documented basis of inflammation is denaturation of protein. One of the parts of this investigation, potency of title benzimidazole-tethered pyrazoles, **6a−6j** to inhibit the denaturation of protein was measured (in triplicate). As a standard drug, diclofenac sodium was utilized in this examination and it provided ∼90% inhibition of protein denaturation. The inhibition percentages of protein denaturation while using the title chemical entities, **6a−6j** are provided in Table 2.

Table 2. Anti-inflammatory Activity of 6a−6j

s. no.	compound	% inhibition
1	**6a**	93.53 ± 1.37
2	**6b**	68.77 ± 1.89
3	**6c**	76.11 ± 0.98
4	**6d**	73.36 ± 2.04
5	**6e**	83.44 ± 2.37
6	**6f**	68.77 ± 1.54
7	**6g**	86.19 ± 1.29
8	**6h**	60.52 ± 1.84
9	**6i**	75.19 ± 1.23
10	**6j**	86.19 ± 1.34
11	DS[a]	90.13 ± 1.45

[a]Diclofenac sodium.

Of all chemical entities investigated, one of them (*i.e.*, **6a**) exhibited superior activity when compared to the standard, whereas two of them (*i.e.*, **6g** and **6j**) exerted ∼95% inhibition when compared to the standard. On the whole, all molecules exhibited good to excellent anti-inflammatory activity and among them, the chemical entity possessing nitro substituent **6a** exerted highest activity when compared with all other molecules investigated and also the activity is superior to that of the standard drug.

2.2.2. Radical Scavenging Activity. In order to determine the radical scavenging activity, a number of techniques including ferric reducing antioxidant power, hydroxyl radical scavenging assay, and organic radical scavenging assay exist. Of those, organic radical scavenging by 2,2-diphenyl-1-picrylhydrazyl (DPPH) is being broadly used by the scientific community around the globe because of its simplicity. In this piece of research, we examined the radical scavenging activity of all synthesized hybrids, **6a−6j** using the method of DPPH.[60] The activity is evaluated in terms of DPPH inhibition (in triplicate), and the outcomes are furnished in Table 3.

As seen in Table 3, all chemical entities exhibited moderate to good radical scavenging potency when compared with the standard ascorbic acid. Of all title benzimidazole-tethered pyrazoles synthesized, the one integrated with the bromo functionality at the para position of one of the aryl groups connected to pyrazole structural motif exerted the highest DPPH inhibition.

Table 3. Radical Scavenging Activity of Target Molecules, 6a−6j

s. no.	molecule	% scavenging	IC_{50} (μM)
1	**6a**	53.22 ± 0.98	94.63
2	**6b**	55.10 ± 1.65	248.80
3	**6c**	50.91 ± 1.34	95.99
4	**6d**	53.81 ± 2.13	121.50
5	**6e**	52.52 ± 1.87	82.41
6	**6f**	46.53 ± 1.23	98.35
7	**6g**	52.80 ± 1.94	21.99
8	**6h**	54.21 ± 1.27	284.50
9	**6i**	64.34 ± 1.95	10.61
10	**6j**	50.34 ± 1.48	34.82
11	AA	88.75 ± 0.89	169.88

2.2.3. Anticancer Activity. Two of the molecular hybrids, **6e** and **6i** were reported as potential therapeutics for human umbilical vein endothelial cell (HUVEC) proliferation.[61] According to the report, HUVEC was used as an antiangiogenesis cell model. However, as our group has been working on the development of a diverse range of heterocyclic molecular hybrids as anticancer agents against pancreatic cancer in the recent years, our aim in this study is to focus on the effects on pancreatic cancer cells. Our transcriptomic study[62] suggested that AsPC1 is a progenitor of human pancreatic cancer cells, whereas SW1990 is a squamous human pancreatic cancer cell line. The inclusion of squamous cancer cells (SW1990) in this study is based on our previous finding suggesting that these cells were more resistant to treatment and had worse prognosis. As a comparison, a progenitor cancer cells (AsPC1) was used.

As a part of this investigation, we have assessed the anticancer evaluation of all synthesized target benzimidazole-tethered pyrazoles, **6a−6j** against human pancreatic cancer cell line AsPCl (progenitor)[62] and SW1990 (squamous)[62] (in triplicate) by adopting a well-known method, CellTiter-Glo luminescent cell viability assay.[62−67] The IC_{50} values of the tested target chemical entities against the human pancreatic cancer cell lines such as SW1990 and AsPC1 as well as non-cancerous cell line, MRC5 are provided in Table 4.

Table 4. Anticancer Activity of Target Chemical Entities, 6a−6j

		IC_{50} (μM)		
s. no.	compound	SW1990	AsPC1	MRC5
1	**6a**	61.8 ± 2.12	>100	>100
2	**6b**	>100	>100	>100
3	**6c**	64.1 ± 1.27	82.5 ± 0.98	>100
4	**6d**	57.6 ± 2.01	62.4 ± 1.65	>100
5	**6e**	>100	>100	>100
6	**6f**	>100	>100	>100
7	**6g**	70.3 ± 0.87	>100	>100
8	**6h**	30.9 ± 0.77	32.8 ± 3.44	80.0 ± 1.19
9	**6i**	>100	>100	>100
10	**6j**	>100	>100	>100
11	gemcitabine	35.09 ± 1.78	39.27 ± 4.44	54.17 ± 0.20

https://dx.doi.org/10.1021/acsomega.0c00630
ACS Omega 2020, 5, 10089−10098

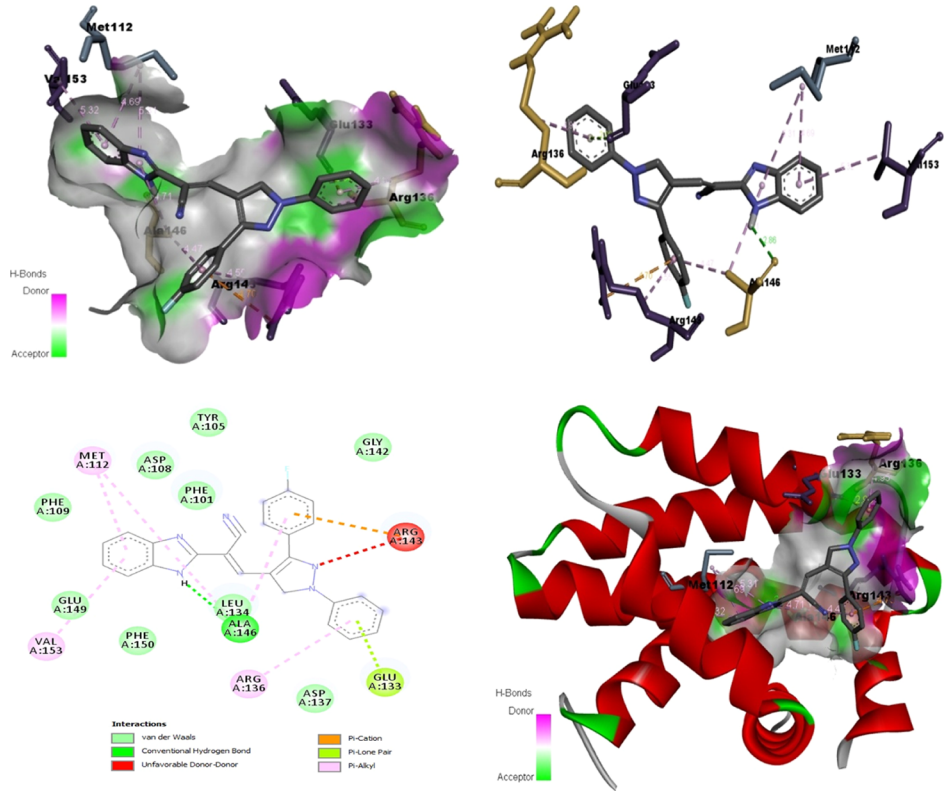

Figure 4. Two- and three-dimensional interactions of BCL-2 with **6h**.

Among all chemical entities tested, **6b**, **6e**, **6f**, **6i** and **6j** exerted IC_{50} values of greater than 100 μM against both cancer cell lines, whereas the rest of the chemical entities exhibited IC_{50} values of less than 100 μM except **6a** against AsPC1, which exhibited greater than 100 μM. Of all, chemical entity **6h** exhibited the best activity against both cancer cell lines. The anticancer activity of all chemical entities against a non-cancerous cell line such as MRC5 was also investigated, and it was observed that the IC_{50} value of the most active chemical entity is much higher than the IC_{50} values against the cancer cell lines. This result clearly implies that the most active chemical entity, the one possessing fluoro substituent on the para position of one of the aryl moiety tethered at pyrazole motif (**6h**) is less toxic.

2.2.4. Molecular Docking. Binding affinity, acquired from the protein data bank, and molecular sources of communications among the active sites of B-cell lymphoma (BCL-2; PDB ID: 4LXD), and the structure of benzimidazole-tethered pyrazole, **6h**, a conformationally stabilized one (three-dimensionally stabilized), were measured through molecular docking studies by employing AutoDock version 4.0. The results gained via docking are furnished in Figure 4. The benzimidazole-tethered pyrazole **6h** exerted its binding energy −8.65 kcal/mol besides its predicted IC_{50} value of 457.41 nM. The molecule, **6h** exhibits van der Waals interactions with phenyl alanine (PHE 101, PHE 109, PHE 150), tyrosine (TYR 105), and leucine (LEU 134), that is amino acids with hydrophobic and aromatic side chains, glutamic acid (GLU 149) and aspartic acid (ASP 108), that is electrically charged acidic amino acids, and glycine (GLY 142), which is a simple hydrophobic amino acid. In addition, conventional hydrogen bond relation between the secondary amino group of the imidazole scaffold and hydrophobic and aliphatic amino acid alanine (ALA 146) was seen. A donor−donor interaction between arginine (ARG 143), an electrically charged and basic amino acid, and a fluoro-containing aromatic ring tethered with pyrazole structural motif, as well as nitrogen at 2-position of pyrazole is noted. In addition, an interaction between carbon and π-of arginine (ARG 143), an electrically charged and basic amino acid, and a fluoro-possessing aromatic moiety, respectively, was also observed. There also exists a π and lone pair interaction between the aromatic nucleus directly linked with the nitrogen of the pyrazole scaffold and glutamic acid (GLU 133), an electrically charged acidic amino acid, respectively. Besides, π−alkyl interactions between fused phenyl ring of the benzimidazole structural motif and amino acids with hydrophobic and aliphatic side chains *viz.*, methionine (MET 112) as well as valine (VAL 153) are noticed. Also, the molecule exhibits π−alkyl interactions between an electrically charged and basic amino acid, arginine (ARG 136) and phenyl moiety integrated with nitrogen of the pyrazole unit as well as an amino acid with hydrophobic and aromatic side chain leucine (LEU 134) and the other aromatic nucleus tethered with the pyrazole scaffold.

3. CONCLUSIONS

A series of heterocyclic hybrids possessing benzimidazole and pyrazole structural motifs, **6a**−**6j** has been synthesized by employing condensation followed by cyclization, formylation, and Knoevenagel reactions. The structure of the hybrids has unequivocally been established based on spectral and physical methods. Of the benzimidazole−pyrazole hybrids, the one possessing the *para*-nitrophenyl moiety connected to a pyrazole ring (**6a**) offered the highest anti-inflammatory activity when evaluated using the protein denaturation method. The evaluation of DPPH radical scavenging activity implies

https://dx.doi.org/10.1021/acsomega.0c00630
ACS Omega 2020, 5, 10089−10098

that the *para*-bromo phenyl structural unit containing the benzimidazole−pyrazole hybrid, **6i** provided the highest activity. Anticancer evaluation by the CellTiter-Glo luminescent cell viability assay technique reflects that among all benzimidazole−pyrazole hybrids, the one tethered with the *para*-fluorophenyl substituent, **6h** exhibited the highest activity against both the human pancreatic cancer cells *viz*., SW1990 and AsPCl with less toxicity. Molecular docking made known significant binding affinity between B-cell lymphoma and the most active hybrid, **6h**. The results reveal that these potent hybrids could serve as competent biological agents and/or be used as competent intermediates to build significant biological agents. Evaluation of anticancer profile of the prominent molecules against various other cancer cell lines, besides constructing hybrids with more structural diversification, hoping to achieve superior outcome, are presently ongoing at our laboratory.

4. EXPERIMENTAL SECTION

4.1. General. All chemicals were purchased from commercial sources. The chemicals used herein are reagent grade and were utilized as-received. All solvents were distilled/dried by employing standard procedures before their utilization. Analytical thin-layer chromatography (TLC) was performed on the precoated TLC sheets of silica gel 60, F_{254} (Merck, Germany) and visualized by long- and short-wavelength UV lamps. Column chromatography was performed on silica gel (spherical, 100−200 mesh) slurry packed in glass columns. The eluent systems used for individual separations are furnished in the respective experimental procedures. All Fourier-transform infrared (FT-IR) spectra in KBr pellets were recorded on a Shimadzu IR Tracer-100 spectrophotometer in the range of 4000−400 cm^{-1}. ^1H and ^{13}C NMR spectra were recorded on an NMR spectrometer (Bruker AVANCE II 400 and 100 MHz) at 25 °C with the use of tetramethylsilane as an internal standard and DMSO-d_6 as the solvent; chemical shifts are expressed in terms of parts per million (δ ppm).

4.2. General Method for the Synthesis of Pyrazole-Based Aldehydes, 4a−4j. A mixture of respective ketones (83.3 mmol) and phenylhydrazine (99.8 mmol) in glacial acetic acid (20 mL) was heated on a water bath for 30 min. The reaction mixture was filtered after cooling and the resulting solid was washed with dilute HCl followed by cold rectified spirit. Recrystallization of the same from ethanol provided the pure respective arylhydrazones, **3a−3j**.[68]

Synthesis of pyrazole-based aldehydes, **4a−4j** was carried out by the application of cold solution of 2 mol VH reagent [dimethylformamide (DMF, 100 mL) − $POCl_3$ (26 mL, 0.28 mol adduct)] in DMF with respective arylhydrazones, **3a−3j**. The reaction mixture was stirred at 70−80 °C for 5−6 h, and it was cooled to room temperature, then poured into cold water. Saturated solution of sodium bicarbonate was then added to neutralize the mixture and the solid thus obtained was filtered, washed with water, and dried to get the aldehydes, **4a−4j**.[68]

4.3. General Method for the Synthesis of Benzimidazole-Tethered Pyrazoles, 6a−6j. A methanolic solution of the respective pyrazole-based aldehydes, **4a−4j** (1 equiv in 10 mL) was added 2-benzimidazoleacetonitrile, **5** (1 equiv) and piperidine (1 equiv). The contents of the flask were refluxed for 2 h, then attaining ambient temperature. The crude thus obtained was poured onto ice pieces and after some time the precipitate was formed. The formed precipitate was filtered and dried. It was then subjected to recrystallization using ethanol to afford pure target molecules, **6a−6j**.

*4.3.1. Synthesis of Benzimidazole-Tethered Pyrazole, **6a**.* A mixture of pyrazole-based aldehyde, **4a** (0.5 g, 1.71 mmol) in methanol (10 mL) was added to 2-benzimidazoleacetonitrile, **5** (0.27 g, 1.71 mmol) and piperidine (0.15 g, 1.71 mmol). After completion of the reaction by adopting the general method, the target molecule, **6a** was obtained. FT-IR (KBr, cm^{-1}) ν: 3305.9, 2218.1, 1595.1, 1521.8, 1423.5, 1348.2, 1232.5, 1109.1, 1068.6, 960.6, 862.2, 817.8, 758.0, 684.7, 636.5, and 497.6; ^1H NMR (400 MHz, DMSO-d_6): δ 9.30 (s, 1H), 8.44 (d, J = 8.8 Hz, 2H), 8.18 (2, 1H), 8.06 (d, J = 8.8 Hz, 2H), 8.00 (d, J = 8 Hz, 2H), 7.65 (t, J = 7.6 Hz, 4H), 7.51 (t, J = 7.2 Hz, 1H), and 7.27−7.24 (m, 2H); ^{13}C NMR (100 MHz, DMSO-d_6): δ 151.8, 148.0, 139.0, 138.0, 135.3, 130.5, 130.4, 129.7, 128.5, 124.6, 123.3, 120.0, 117.0, and 116.3; Anal. Calcd for $C_{25}H_{16}N_6O_2$ (%): C, 69.44; H, 3.73; N, 19.43. Found: C, 69.52; H, 3.79; N, 19.37.

*4.3.2. Synthesis of Benzimidazole-Tethered Pyrazole, **6b**.* A mixture of pyrazole-based aldehyde, **4b** (0.5 g, 1.58 mmol), 2-benzimidazoleacetonitrile **5** (0.25 g, 1.58 mmol), and piperidine (0.13 g, 1.58 mmol) in methanol (10 mL), after completion of the reaction by adopting the general method, provide the target molecule, **6b**. FT-IR (KBr, cm^{-1}) ν: 3290.4, 2240.1, 1600.7, 1531.3, 1418.1, 1355.3, 1244.5, 1111.2, 1052.7, 969.6, 856.5, 813.3, 757.0, 677.7, 663.5, 635.3, and 497.6; ^1H NMR (400 MHz, DMSO-d_6): δ 9.25 (s, 1H), 7.95−7.92 (m, 3H), 7.82 (s, 1H), 7.70−7.59 (m, 6H), 7.47 (t, J = 7.6 Hz, 1H), and 7.24−7.22 (m, 2H); ^{13}C NMR (100 MHz, DMSO-d_6): δ 151.7, 147.7, 139.0, 135.6, 134.4, 130.4, 130.1, 129.5, 128.4, 128.3, 128.2, 123.3, 119.9, 117.2, and 117.1; Anal. Calcd for $C_{25}H_{15}Cl_2N_5$ (%): C, 65.80; H, 3.31; N, 15.35. Found: C, 65.91; H, 3.25; N, 15.28.

*4.3.3. Synthesis of Benzimidazole-Tethered Pyrazole, **6c**.* A mixture of pyrazole-based aldehyde, **4c** (0.5 g, 1.53 mmol) in methanol (10 mL) was added to 2-benzimidazoleacetonitrile, **5** (0.24 g, 1.53 mmol) and piperidine (0.13 g, 1.53 mmol). After completion of the reaction by adopting the general method, the target molecule, **6c** was obtained. FT-IR (KBr, cm^{-1}): δ 3345.6, 3085.6, 2236.2, 1599.2, 1544.4, 1526.5, 1444.6, 1435.7, 1362.3, 1327.7, 1243.4, 1180.4, 1089.8, 1056.9, 1012.6, 950.9, 923.9, 840.9, 813.9, 795.0, 745.7, 679.9, 638.4, 615.6, 585.6, and 546.8; ^1H NMR (400 MHz, DMSO-d_6): δ 9.25 (s, 1H), 8.15 (s, 1H), 7.96 (t, J = 8 Hz, 3H), 7.78−7.71 (m, 2H), 7.64−7.54 (m, 5H), 7.47 (t, J = 7.2 Hz, 1H), and 7.26−7.23 (m, 2H); ^{13}C NMR (100 MHz, DMSO-d_6): δ 152.6, 147.8, 139.1, 135.6, 133.9, 132.3, 131.6, 130.3, 129.2, 128.6, 128.3, 123.3, 122.7, 119.9, 117.1, and 115.9; Anal. Calcd for $C_{25}H_{16}BrN_5$ (%): C, 64.39; H, 3.46; N, 15.02. Found: C, 64.46; H, 3.50; N, 15.09.

*4.3.4. Synthesis of Benzimidazole-Tethered Pyrazole, **6d**.* A mixture of pyrazole-based aldehyde, **4d** (0.5 g, 1.78 mmol), 2-benzimidazoleacetonitrile, **5** (0.28 g, 1.78 mmol), and piperidine (0.15 g, 1.78 mmol) in methanol (10 mL), after completion of the reaction by adopting the general method, gave the target molecule, **6d**. FT-IR (KBr, cm^{-1}) ν: 3335.6, 3085.6, 2935.4, 2884.3, 2245.3, 1601.2, 1548.2, 1530.5, 1447.7, 1438.4, 1370.3, 1330.4, 1250.4, 1175.4, 1090.4, 1065.2, 1012.6, 950.9, 923.9, 840.9, 813.9, 795.0, 754.2, 680.9, 640.3, 620.4, and 585.6; ^1H NMR (400 MHz, DMSO-d_6): δ 9.22 (s, 1H), 8.14 (s, 1H), 7.95 (d, J = 7.6 Hz, 2H), 7.67−7.59 (m, 6H), 7.45 (t, J = 7.6 Hz, 1H), 7.25−7.22 (m, 2H), 7.15 (d, J = 8.8 Hz, 2H), and 3.86 (s, 3H); ^{13}C NMR (100 MHz, DMSO-d_6):

https://dx.doi.org/10.1021/acsomega.0c00630
ACS Omega 2020, 5, 10089−10098

δ 160.4, 154.2, 147.9, 139.2, 136.2, 130.7, 130.6, 130.3, 128.8, 128.1, 123.9, 123.2, 119.8, 119.4, 118.8, 117.3, 115.6, 114.9, 114.8, 114.5, and 55.7; Anal. Calcd for $C_{26}H_{19}N_5O$ (%): C, 74.80; H, 4.59; N, 16.78. Found: C, 74.91; H, 4.51; N, 16.73.

4.3.5. Synthesis of Benzimidazole-Tethered Pyrazole, ***6e****.* A mixture of pyrazole-based aldehyde, **4e** (0.5 g, 1.77 mmol) in methanol (10 mL) was added to 2-benzimidazoleacetonitrile, **5** (0.28 g, 1.77 mmol) and piperidine (0.15 g, 1.77 mmol). After completion of the reaction by adopting the general method, it provided the target molecule, **6e**. FT-IR (KBr, cm^{-1}) ν: 3290.4, 2220.1, 1600.7, 1531.3, 1418.1, 1355.3, 1244.5, 1111.2, 1067.7, 975.5, 865.2, 810.5, 757.2, 685.7, 663.5, 655.3, and 458.6; ^{1}H NMR (400 MHz, DMSO-d_6): δ 9.25 (s, 1H), 8.12 (s, 1H), 7.96 (d, J = 7.6 Hz, 2H), 7.76 (d, J = 8.4 Hz, 2H), 7.67−7.60 (m, 6H), 7.47 (t, J = 7.6 Hz, 1H), and 7.26−7.24 (m, 2H); ^{13}C NMR (100 MHz, DMSO-d_6): δ 153.1, 147.8, 139.1, 135.7, 134.4, 131.1, 130.8, 130.4, 130.3, 129.5, 129.3, 129.2, 128.3, 123.3, 119.9, 117.1, and 115.8; Anal. Calcd for $C_{25}H_{16}ClN_5$ (%): C, 71.17; H, 3.82; N, 16.60. Found: C, 71.26; H, 3.87; N, 16.55.

4.3.6. Synthesis of Benzimidazole-Tethered Pyrazole, ***6f****.* A mixture of pyrazole-based aldehyde, **4f** (0.5 g, 1.91 mmol), 2-benzimidazoleacetonitrile, **5** (0.30 g, 1.91 mmol), and piperidine (0.16 g, 1.91 mmol) in methanol (10 mL), after completion of the reaction by adopting the general method, furnished the target molecule, **6f**. FT-IR (KBr, cm^{-1}) ν: 3295.4, 2190.5, 1705.6, 1600.7, 1531.3, 1418.1, 1368.5, 1355.3, 1244.5, 1111.2, 1052.7, 969.6, 856.5, 813.3, 757.0, 677.7, 663.5, 635.3, and 497.6; ^{1}H NMR (400 MHz, DMSO-d_6): δ 9.23 (s, 1H), 8.14 (s, 1H), 7.95 (d, J = 7.6 Hz, 2H), 7.63−7.59 (m, 6H), 7.48−7.44 (m, 1H), 7.42−7.40 (m, 2H), 7.25−7.22 (m, 2H), and 2.42 (s, 3H); ^{13}C NMR (100 MHz, DMSO-d_6): δ 154.4, 147.8, 139.2, 139.1, 136.2, 130.3, 130.0, 129.3, 128.9, 128.7, 128.1, 123.2, 119.8, 117.2, and 21.3; Anal. Calcd for $C_{26}H_{19}N_5$ (%): C, 77.79; H, 4.77; N, 17.44. Found: C, 77.89; H, 4.70; N, 17.49.

4.3.7. Synthesis of Benzimidazole-Tethered Pyrazole, ***6g****.* To a mixture of pyrazole-based aldehyde, **4g** (0.5 g, 1.77 mmol) in methanol (10 mL), were added 2-benzimidazoleacetonitrile, **5** (0.28 g, 1.77 mmol) and piperidine (0.15 g, 1.77 mmol). After completion of the reaction by adopting the general method, it gave the target molecule, **6g**. FT-IR (KBr, cm^{-1}) ν: 3323.4, 2212.4, 1589.3, 1525.7, 1498.7, 1415.8, 1355.9, 1305.8, 1271.1, 1240.2, 1078.2, 954.8, 918.1, 817.8, 756.1, 736.8, 680.9, 650.0, 609.5, 574.8, 513.1, 470.6, and 439.8; ^{1}H NMR (400 MHz, DMSO-d_6): δ 9.25 (s, 1H), 8.15 (s, 1H), 7.96 (t, J = 8 Hz, 3H), 7.78−7.72 (m, 2H), 7.64−7.54 (m, 5H), 7.47 (t, J = 7.6 Hz, 1H), and 7.26−7.24 (m, 2H); ^{13}C NMR (100 MHz, DMSO-d_6): δ 152.6, 147.8, 139.1, 135.6, 133.9, 132.3, 131.6, 130.3, 129.2, 128.6, 128.3, 123.3, 122.7, 119.9, 117.1, and 115.9; Anal. Calcd for $C_{25}H_{16}ClN_5$ (%): C, 71.17; H, 3.82; N, 16.60. Found: C, 71.29; H, 3.87; N, 16.54.

4.3.8. Synthesis of Benzimidazole-Tethered Pyrazole, ***6h****.* A mixture of pyrazole-based aldehyde, **4h** (0.5 g, 1.88 mmol) (10 mL), 2-benzimidazoleacetonitrile, **5** (0.29 g, 1.88 mmol), and piperidine (0.16 g, 1.71 mmol) in methanol (10 mL), after the completion of the reaction by adopting the general method, offered the target molecule, **6h**. FT-IR (KBr, cm^{-1}) ν: 3300.2, 3062.9, 2216.2, 1595.1, 1533.4, 1508.3, 1446.6, 1417.7, 1354.0, 1307.7, 1273.0, 1153.4, 1089.8, 1056.9, 1012.6, 950.9, 923.9, 840.9, 813.9, 785.0, 738.7, 680.9, 638.4, and 607.6; ^{1}H NMR (400 MHz, DMSO-d_6): δ 9.24 (s, 1H), 8.12 (s, 1H), 7.96 (d, J = 8 Hz, 2H), 7.81−7.77 (m, 2H), 7.64−7.58 (m, 4H), 7.49−7.42 (m, 3H), and 7.25−7.23 (m, 2H); ^{13}C NMR (100 MHz, DMSO-d_6): δ 164.4, 161.9, 153.3, 147.8, 139.1, 135.9, 131.5, 130.3, 129.1, 128.2, 128.1, 123.3, 119.9, 117.2, 116.5, 116.3, and 115.8; Anal. Calcd for $C_{25}H_{16}FN_5$ (%): C, 74.06; H, 3.98; N, 17.27. Found: C, 74.19; H, 3.92; N, 17.20.

4.3.9. Synthesis of Benzimidazole-Tethered Pyrazole, ***6i****.* To a mixture of pyrazole-based aldehyde, **4i** (0.5 g, 1.53 mmol) in methanol (10 mL) were added 2-benzimidazoleacetonitrile, **5** (0.24 g, 1.53 mmol) and piperidine (0.13 g, 1.53 mmol). After completion of the reaction by adopting the general method, it offered the target molecule, **6i**. FT-IR (KBr, cm^{-1}) ν: 3326.6, 3094.6, 2250.2, 1595.6, 1544.4, 1526.5, 1462.6, 1453.1, 1362.3, 1327.7, 1243.4, 1180.4, 1098.5, 1056.9, 1017.3, 955.5, 932.7, 844.9, 825.7, 795.0, 745.7, 679.9, 647.4, 625.6, 577.8, and 534.2; ^{1}H NMR (400 MHz, DMSO-d_6): δ 9.25 (s, 1H), 8.13 (s, 1H), 7.96 (d, J = 8 Hz, 2H), 7.80 (d, J = 8.4 Hz, 2H), 7.70 (d, J = 8.4 Hz, 2H), 7.63−7.60 (m, 4H), 7.49−7.45 (m, 1H), and 7.26−7.24 (m, 2H); ^{13}C NMR (100 MHz, DMSO-d_6): δ 153.1, 147.7, 139.1, 135.7, 132.4, 131.4, 130.8, 130.0, 129.2, 128.3, 123.1, 119.9, 117.1, and 115.8; Anal. Calcd for $C_{25}H_{16}BrN_5$ (%): C, 64.39; H, 3.46; N, 15.02. Found: C, 64.48; H, 3.53; N, 14.95.

4.3.10. Synthesis of Benzimidazole-Tethered Pyrazole, ***6j****.* A mixture of pyrazole-based aldehyde, **4j** (0.5 g, 2.0 mmol), 2-benzimidazoleacetonitrile, **5** (0.32 g, 2.0 mmol), and piperidine (0.17 g, 2.0 mmol) in methanol (10 mL), after completion of the reaction by adopting the general method, provided the target molecule, **6j**. FT-IR (KBr, cm^{-1}) ν: 3304.1, 3061.0, 2216.2, 1593.2, 1531.5, 1502.6, 1444.7, 1419.6, 1361.7, 1305.8, 1274.9, 1242.2, 954.8, 921.9, 817.8, 777.3, 702.1, 678.9, 634.6, 609.5, 582.5, and 513.1; ^{1}H NMR (400 MHz, DMSO-d_6): δ 9.25 (s, 1H), 8.17 (s, 1H), 7.96 (d, J = 8 Hz, 2H), 7.74 (d, J = 6.4 Hz, 2H), 7.64−7.54 (m, 7H), 7.48−7.45 (m, 1H), and 7.25−7.23 (m, 2H); ^{13}C NMR (100 MHz, DMSO-d_6): δ 154.3, 147.8, 139.2, 136.1, 131.6, 130.3, 129.5, 129.4, 129.3, 129.1, 128.2, 123.3, 119.9, 117.2, and 115.8; Anal. Calcd for $C_{25}H_{17}N_5$ (%): C, 77.50; H, 4.42; N, 18.08. Found: C, 77.59; H, 4.46; N, 18.02.

4.4. Anti-inflammatory Activity by Protein Denaturation Method. With minor modification, the Mizushima and Kobayashi[59] method has been utilized to evaluate the anti-inflammatory (*in vitro*) activity. The reaction mixture (2.5 mL) is molecules (1 mL; 1 mM), phosphate buffered saline (PBS, 1.4 mL; pH 6.4), and egg albumin (0.1 mL). The control used was double distilled water (equal volume). After incubation at 37 °C ± 2 for 15 min, the content was then heated at 70 °C for 5 min. Their absorbance, after attaining ambient temperature, was noted at 660 nm using vehicle as blank. As a reference drug, diclofenac sodium (1 mM) was utilized and treated alike to determine the absorbance. The percentage inhibition of protein denaturation was calculated by applying the following equation.

$$\text{Inhibition (\%) of protein denaturation} = \frac{\text{AC} - \text{AS}}{\text{AC}} \times 100$$

where AC—absorbance of control, AS—absorbance of sample.

4.5. Radical Scavenging Activity by DPPH Method. The assay of radical scavenging (DPPH) was carried out as per the literature method[60] with slight modification. DPPH (1.6 mg) was dissolved in DMSO (50 mL). DPPH solution (1.5 mL) was added to each molecule prepared (1.5 mL; 100 μg/mL) and set aside for 45 min incubation at ambient temperature under dark condition. The absorbance variations

https://dx.doi.org/10.1021/acsomega.0c00630
ACS Omega 2020, 5, 10089−10098

at 517 nm were then measured. The blank DPPH solution (absorbance at 517 nm) was used as the control. The DPPH free-radical scavenging activity was calculated by using the equation mentioned below

$$\text{Radical scavenging (\%)} = \frac{\text{AC} - \text{AS}}{\text{AC}} \times 100$$

where AC—absorbance of control, AS—absorbance of sample.

4.6. Anticancer Evaluation. The AsPC1 and SW1990 (human pancreatic cancer cells) were acquired from the American Type Culture Collection (ATCC), USA. RPMI–fetal bovine serum medium supplemented with 100 IU/mL of penicillin and 100 μg/mL of streptomycin (Sigma-Aldrich, St. Louis, MO, USA) was used to culture all cells. The cells were incubated at 37 °C in 5% CO_2, utilizing the established standard *in vitro* cell culture method.[62−65]

To assess antitumor effects of the synthesized molecules, stock solutions of the same in DMSO (100 mM) were first prepared, then further diluted to 0.1 mM in sterile PBS. The cells were treated based on the reported method of cell viability assay. Initially, 384-well plates were seeded with the cells (1500 cells/well). The plates were incubated for 24 h. And then the cells were treated with the molecules synthesized for 72 h. Cell viability was recorded using the CellTiter-Glo luminescent cell viability assay (Promega, USA). The luminescence readings were measured using a SpectraMax M3 microplate reader (Molecular Devices Corporation, USA).

AUTHOR INFORMATION

Corresponding Author

Chennan Ramalingan − *Department of Chemistry, School of Advanced Sciences, Kalasalingam Academy of Research and Education (Deemed to be University), Krishnankoil 626 126, Tamilnadu, India;* orcid.org/0000-0002-1585-9542; Email: ramalinganc@gmail.com

Authors

Ramar Sivaramakarthikeyan − *Department of Chemistry, School of Advanced Sciences, Kalasalingam Academy of Research and Education (Deemed to be University), Krishnankoil 626 126, Tamilnadu, India*

Shunmugam Iniyaval − *Department of Chemistry, School of Advanced Sciences, Kalasalingam Academy of Research and Education (Deemed to be University), Krishnankoil 626 126, Tamilnadu, India*

Vadivel Saravanan − *Department of Chemistry, School of Advanced Sciences, Kalasalingam Academy of Research and Education (Deemed to be University), Krishnankoil 626 126, Tamilnadu, India*

Wei-Meng Lim − *School of Pharmacy, International Medical University, Kuala Lumpur 57000, Malaysia*

Chun-Wai Mai − *School of Pharmacy and Center for Cancer and Stem Cell Research, Institute for Research, Development and Innovation (IRDI), International Medical University, Kuala Lumpur 57000, Malaysia*

Complete contact information is available at: https://pubs.acs.org/10.1021/acsomega.0c00630

Notes

The authors declare no competing financial interest.

ACKNOWLEDGMENTS

Financial assistance provided by the Indian Council of Medical Research, New Delhi, India (no. 58/16/2013BMS) is gratefully acknowledged.

REFERENCES

(1) https://www.who.int/news-room/fact-sheets, 2018 (accessed 2018-09-12).

(2) Niederhuber, J. E.; Brennan, M. F.; Menck, H. R. The national cancer data base report on pancreatic cancer. *Cancer* **1995**, *76*, 1671−1677.

(3) Rawla, P.; Sunkara, T.; Gaduputi, V. Epidemiology of pancreatic cancer: global trends, etiology and risk factors. *World J. Oncol.* **2019**, *10*, 10−27.

(4) Hernández-Covarrubias, C.; Vilchis-Reyes, M. A.; Yépez-Mulia, L.; Sánchez-Díaz, R.; Navarrete-Vázquez, G.; Hernández-Campos, A.; Castillo, R.; Hernández-Luis, F. Exploring the interplay of physicochemical properties, membrane permeability and giardicidal activity of some benzimidazole derivatives. *Eur. J. Med. Chem.* **2012**, *52*, 193−204.

(5) Akhtar, M. J.; Khan, A. A.; Ali, Z.; Dewangan, R. P.; Rafi, M.; Hassan, M. Q.; Akhtar, M. S.; Siddiqui, A. A.; Partap, S.; Pasha, S.; Yar, M. S. Synthesis of stable benzimidazole derivatives bearing pyrazole as anticancer and EGFR receptor inhibitors. *Bioorg. Chem.* **2018**, *78*, 158−169.

(6) Lavrador-Erb, K.; Ravula, S. B.; Yu, J.; Zamani-Kord, S.; Moree, W. J.; Petroski, R. E.; Wen, J.; Malany, S.; Hoare, S. R. J.; Madan, A.; Crowe, P. D.; Beaton, G. The discovery and structure-activity relationships of 2-(piperidin-3-yl)-1H-benzimidazoles as selective, CNS penetrating H1-antihistamines for insomnia. *Bioorg. Med. Chem. Lett.* **2010**, *20*, 2916−2919.

(7) Tahlan, S.; Narasimhan, B.; Lim, S. M.; Ramasamy, K.; Mani, V.; Shah, S. A. A. 2-Mercaptobenzimidazole schiff bases: design, synthesis, antimicrobial studies and anticancer activity on HCT-116 cell line. *Mini-Rev. Med. Chem.* **2019**, *19*, 1080−1092.

(8) Kuş, C.; Ayhan-Kilcigil, G.; Özbey, S.; Betül Kaynak, F.; Kaya, M.; Çoban, T.; Can-Eke, B. Synthesis and antioxidant properties of novel N-methyl-1,3,4-thiadiazol-2-amine and 4-methyl-2H-1,2,4-triazole-3(4H)-thione derivatives of benzimidazole class. *Bioorg. Med. Chem.* **2008**, *16*, 4294−4303.

(9) Galal, S. A.; Abdelsamie, A. S.; Shouman, S. A.; Attia, Y. M.; Ali, H. I.; Tabll, A.; El-Shenawy, R.; El Abd, Y. S.; Ali, M. M.; Mahmoud, A. E.; Abdel-Halim, A. H.; Fyiad, A. A.; Girgis, A. S.; El-Diwani, H. I. Part I: Design, synthesis and biological evaluation of novel pyrazole-benzimidazole conjugates as checkpoint kinase 2 (Chk2) inhibitors with studying their activities alone and in combination with genotoxic drugs. *Eur. J. Med. Chem.* **2017**, *134*, 392−405.

(10) Zhang, J.; Wang, J.-L.; Zhou, Z.-M.; Li, Z.-H.; Xue, W.-Z.; Xu, D.; Hao, L.-P.; Han, X.-F.; Fei, F.; Liu, T.; Liang, A.-H. Design, synthesis and biological activity of 6-substituted carbamoyl benzimidazoles as new nonpeptidic angiotensin II AT1 receptor antagonists. *Bioorg. Med. Chem.* **2012**, *20*, 4208−4216.

(11) Patil, A.; Ganguly, S.; Surana, S. Synthesis and antiulcer activity of 2-[5-substituted-1-H-benzo(d) imidazol-2-yl sulfinyl]methyl-3-substituted quinazoline-4-(3H) ones. *J. Chem. Sci.* **2010**, *122*, 443−450.

(12) Galal, S. A.; Khattab, M.; Shouman, S. A.; Ramadan, R.; Kandil, O. M.; Kandil, O. M.; Tabll, A.; El Abd, Y. S.; El-Shenawy, R.; Attia, Y. M.; El-Rashedy, A. A.; El Diwani, H. I. Part III: Novel checkpoint kinase 2 (Chk2) inhibitors; design, synthesis and biological evaluation of pyrimidine-benzimidazole conjugates. *Eur. J. Med. Chem.* **2018**, *146*, 687−708.

(13) Shrivastava, N.; Naim, M. J.; Alam, M. J.; Nawaz, F.; Ahmed, S.; Alam, O. Benzimidazole scaffold as anticancer agent: synthetic approaches and structure−activity relationship. *Arch. Pharm.* **2017**, *350*, e201700040.

(14) Keri, R. S.; Hiremathad, A.; Budagumpi, S.; Nagaraja, B. M. Comprehensive review in current developments of benzimidazole-based medicinal chemistry. *Chem. Biol. Drug Des.* **2015**, *86*, 19−65.
(15) Yadav, G.; Ganguly, S. Structure activity relationship (SAR) study of benzimidazole scaffold for different biological activities: A mini-review. *Eur. J. Med. Chem.* **2015**, *97*, 419−443.
(16) Gaba, M.; Mohan, C. Development of drugs based on imidazole and benzimidazole bioactive heterocycles: recent advances and future directions. *Med. Chem. Res.* **2016**, *25*, 173−210.
(17) Gaba, M.; Singh, S.; Mohan, C. Benzimidazole: An emerging scaffold for analgesic and anti-inflammatory agents. *Eur. J. Med. Chem.* **2014**, *76*, 494−505.
(18) DeSimone, R.; Currie, K.; Mitchell, S.; Darrow, J.; Pippin, D. Privileged structures: applications in drug discovery. *Comb. Chem. High Throughput Screening* **2004**, *7*, 473−493.
(19) Tageja, N.; Nagi, J. Bendamustine: something old, something new. *Cancer Chemother. Pharmacol.* **2010**, *66*, 413−423.
(20) Cheson, B. D.; Rummel, M. J. Bendamustine: rebirth of an old drug. *J. Clin. Oncol.* **2009**, *27*, 1492−1501.
(21) Cheson, B. D.; Brugger, W.; Damaj, G.; Dreyling, M.; Kahl, B.; Kimby, E.; Ogura, M.; Weidmann, E.; Wendtner, C.-M.; Zinzani, P. L. Optimal use of bendamustine in hematologic disorders: Treatment recommendations from an international consensus panel - an update. *Leuk. Lymphoma* **2016**, *57*, 766−782.
(22) Njar, V. C. O.; Brodie, A. M. H. Discovery and development of galeterone (TOK-001 or VN/124-1) for the treatment of all stages of prostate cancer. *J. Med. Chem.* **2015**, *58*, 2077−2087.
(23) Ansari, A.; Ali, A.; Asif, M.; Shamsuzzaman, S. Review: biologically active pyrazole derivatives. *New J. Chem.* **2017**, *41*, 16−41.
(24) Fustero, S.; Sánchez-Roselló, M.; Barrio, P.; Simón-Fuentes, A. From 2000 to mid-2010: A fruitful decade for the synthesis of pyrazoles. *Chem. Rev.* **2011**, *111*, 6984−7034.
(25) Keter, F. K.; Darkwa, J. Perspective: the potential of pyrazole-based compounds in medicine. *BioMetals* **2012**, *25*, 9−21.
(26) Kumar, V.; Kaur, K.; Gupta, G. K.; Sharma, A. K. Pyrazole containing natural products: synthetic preview and biological significance. *Eur. J. Med. Chem.* **2013**, *69*, 735−753.
(27) Galal, S. A.; Khairat, S. H. M.; Ali, H. I.; Shouman, S. A.; Attia, Y. M.; Ali, M. M.; Mahmoud, A. E.; Abdel-Halim, A. H.; Fyiad, A. A.; Tabll, A.; El-Shenawy, R.; El Abd, Y. S.; Ramdan, R.; El Diwani, H. I. Part II: New candidates of pyrazole-benzimidazole conjugates as checkpoint kinase 2 (Chk2) inhibitors. *Eur. J. Med. Chem.* **2018**, *144*, 859−873.
(28) Reddy, T. S.; Kulhari, H.; Reddy, V. G.; Bansal, V.; Kamal, A.; Shukla, R. Design, synthesis and biological evaluation of 1,3-diphenyl-1H-pyrazole derivatives containing benzimidazole skeleton as potential anticancer and apoptosis inducing agents. *Eur. J. Med. Chem.* **2015**, *101*, 790−805.
(29) Karrouchi, K.; Radi, S.; Ramli, Y.; Taoufik, J.; Mabkhot, Y.; Al-aizari, F.; Ansar, M. h. Synthesis and pharmacological activities of pyrazole derivatives: a review. *Molecules* **2018**, *23*, 134.
(30) Zheng, L.-W.; Shao, J.-H.; Zhao, B.-X.; Miao, J.-Y. Synthesis of novel pyrazolo[1,5-a]pyrazin-4(5H)-one derivatives and their inhibition against growth of A549 and H322 lung cancer cells. *Bioorg. Med. Chem. Lett.* **2011**, *21*, 3909−3913.
(31) Liu, Y.-R.; Luo, J.-Z.; Duan, P.-P.; Shao, J.; Zhao, B.-X.; Miao, J.-Y. Synthesis of pyrazole peptidomimetics and their inhibition against A549 lung cancer cells. *Bioorg. Med. Chem. Lett.* **2012**, *22*, 6882−6887.
(32) Farag, A. M.; Mayhoub, A. S.; Barakat, S. E.; Bayomi, A. H. Regioselective synthesis and antitumor screening of some novel N-phenylpyrazole derivatives. *Bioorg. Med. Chem.* **2008**, *16*, 881−889.
(33) Huang, Y.-Y.; Wang, L.-Y.; Chang, C.-H.; Kuo, Y.-H.; Kaneko, K.; Takayama, H.; Kimura, M.; Juang, S.-H.; Wong, F. F. One-pot synthesis and antiproliferative evaluation of pyrazolo[3,4-d]-pyrimidine derivatives. *Tetrahedron* **2012**, *68*, 9658−9664.
(34) Li, X.; Lu, X.; Xing, M.; Yang, X.-H.; Zhao, T.-T.; Gong, H.-B.; Zhu, H.-L. Synthesis, biological evaluation, and molecular docking studies of N,1,3-triphenyl-1H-pyrazole-4-carboxamide derivatives as anticancer agents. *Bioorg. Med. Chem. Lett.* **2012**, *22*, 3589−3593.
(35) Strocchi, E.; Fornari, F.; Minguzzi, M.; Gramantieri, L.; Milazzo, M.; Rebuttini, V.; Breviglieri, S.; Camaggi, C. M.; Locatelli, E.; Bolondi, L.; Comes-Franchini, M. Design, synthesis and biological evaluation of pyrazole derivatives as potential multi-kinase inhibitors in hepatocellular carcinoma. *Eur. J. Med. Chem.* **2012**, *48*, 391−401.
(36) Sun, J.; Lv, X.-H.; Qiu, H.-Y.; Wang, Y.-T.; Du, Q.-R.; Li, D.-D.; Yang, Y.-H.; Zhu, H.-L. Synthesis, biological evaluation and molecular docking studies of pyrazole derivatives coupling with a thiourea moiety as novel CDKs inhibitors. *Eur. J. Med. Chem.* **2013**, *68*, 1−9.
(37) Abd El-Karim, S. S.; Anwar, M. M.; Mohamed, N. A.; Nasr, T.; Elseginy, S. A. Design, synthesis, biological evaluation and molecular docking studies of novel benzofuran-pyrazole derivatives as anticancer agents. *Bioorg. Chem.* **2015**, *63*, 1−12.
(38) Alam, R.; Wahi, D.; Singh, R.; Sinha, D.; Tandon, V.; Grover, A.; Rahisuddin. Design, synthesis, cytotoxicity, HuTopoIIα inhibitory activity and molecular docking studies of pyrazole derivatives as potential anticancer agents. *Bioorg. Chem.* **2016**, *69*, 77−90.
(39) Puddefoot, J. R.; Barker, S.; Glover, H. R.; Malouitre, S. D. M.; Vinson, G. P. Non-competitive steroid inhibition of oestrogen receptor functions. *Int. J. Cancer* **2002**, *101*, 17−22.
(40) He, H.; Tran, P.; Yin, H.; Smith, H.; Batard, Y.; Wang, L.; Einolf, H.; Gu, H.; Mangold, J. B.; Fischer, V.; Howard, D. Absorption, metabolism, and excretion of [^{14}C]vildagliptin, a novel dipeptidyl peptidase 4 inhibitor, in humans. *Drug Metab. Dispos.* **2009**, *37*, 536−544.
(41) Royer, R. E.; Deck, L. M.; Campos, N. M.; Hunsaker, L. A.; Vander Jagt, D. L. Biologically active derivatives of gossypol: synthesis and antimalarial activities of peri-acylated gossylic nitriles. *J. Med. Chem.* **1986**, *29*, 1799−1801.
(42) Koga, H.; Nanjoh, Y.; Makimura, K.; Tsuboi, R. In vitro antifungal activities of luliconazole, a new topical imidazole. *Med. Mycol.* **2009**, *47*, 640−647.
(43) Niwano, Y.; Ohmi, T.; Seo, A.; Kodama, H.; Koga, H.; Sakai, A. Lanoconazole and its related optically active compound NND-502: novel antifungal imidazoles with a ketene dithioacetal structure. *Curr. Med. Chem.: Anti-Infect. Agents* **2003**, *2*, 147−160.
(44) Murphy, S. T.; Case, H. L.; Ellsworth, E.; Hagen, S.; Huband, M.; Joannides, T.; Limberakis, C.; Marotti, K. R.; Ottolini, A. M.; Rauckhorst, M.; Starr, J.; Stier, M.; Taylor, C.; Zhu, T.; Blaser, A.; Denny, W. A.; Lu, G.-L.; Smaill, J. B.; Rivault, F. The synthesis and biological evaluation of novel series of nitrile-containing fluoroquinolones as antibacterial agents. *Bioorg. Med. Chem. Lett.* **2007**, *17*, 2150−2155.
(45) Laurence, C.; Brameld, K. A.; Graton, J.; Le Questel, J.-Y.; Renault, E. The pKBHX database: toward a better understanding of hydrogen-bond basicity for medicinal chemists. *J. Med. Chem.* **2009**, *52*, 4073−4086.
(46) Viegas-Junior, C.; Danuello, A.; Bolzani, V. D. S.; Barreiro, E. J.; Fraga, C. A. M. Molecular hybridization: a useful tool in the design of new drug prototypes. *Curr. Med. Chem.* **2007**, *14*, 1829−1852.
(47) Gediya, L. K.; Njar, V. C. Promise and challenges in drug discovery and development of hybrid anticancer drugs. *Expert Opin. Drug Discovery* **2009**, *4*, 1099−1111.
(48) Milik, S. N.; Lasheen, D. S.; Serya, R. A. T.; Abouzid, K. A. M. How to train your inhibitor: design strategies to overcome resistance to epidermal growth factor receptor inhibitors. *Eur. J. Med. Chem.* **2017**, *142*, 131−151.
(49) Zhu, D.; Huang, H.; Pinkas, D. M.; Luo, J.; Ganguly, D.; Fox, A. E.; Arner, E.; Xiang, Q.; Tu, Z.-C.; Bullock, A. N.; Brekken, R. A.; Ding, K.; Lu, X. 2-Amino-2,3-dihydro-1H-indene-5-carboxamide-based discoidin domain receptor 1 (DDR1) inhibitors: design, synthesis, and in vivo antipancreatic cancer efficacy. *J. Med. Chem.* **2019**, *62*, 7431−7444.
(50) Salem, M. S. H.; Abdel Aziz, Y. M.; Elgawish, M. S.; Said, M. M.; Abouzid, K. A. M. Design, synthesis, biological evaluation and molecular modeling study of new thieno[2,3-d]pyrimidines with anti-

https://dx.doi.org/10.1021/acsomega.0c00630
ACS Omega 2020, 5, 10089−10098

proliferative activity on pancreatic cancer cell lines. *Bioorg. Chem.* **2020**, *94*, 103472.
(51) Bozdag, M.; Ferraroni, M.; Ward, C.; Carta, F.; Bua, S.; Angeli, A.; Langdon, S. P.; Kunkler, I. H.; Al-Tamimi, A.-M. S.; Supuran, C. T. Carbonic anhydrase inhibitors based on sorafenib scaffold: design, synthesis, crystallographic investigation and effects on primary breast cancer cells. *Eur. J. Med. Chem.* **2019**, *182*, 111600.
(52) Bayrak, N.; Yıldırım, H.; Yıldız, M.; Radwan, M. O.; Otsuka, M.; Fujita, M.; Tuyun, A. F.; Ciftci, H. I. Design, synthesis, and biological activity of plastoquinone analogs as a new class of anticancer agents. *Bioorg. Chem.* **2019**, *92*, 103255.
(53) Mohan, C. D.; Srinivasa, V.; Rangappa, S.; Mervin, L.; Mohan, S.; Paricharak, S.; Baday, S.; Li, F.; Shanmugam, M. K.; Chinnathambi, A.; Zayed, M. E.; Alharbi, S. A.; Bender, A.; Sethi, G.; Basappa; Rangappa, K. S. Trisubstituted-imidazoles induce apoptosis in human breast cancer cells by targeting the oncogenic PI3K/Akt/mTOR signaling pathway. *PLoS One* **2016**, *11*, e0153155.
(54) Shaw, A. Y.; Liau, H.-H.; Lu, P.-J.; Yang, C.-N.; Lee, C.-H.; Chen, J.-Y.; Xu, Z.; Flynn, G. 3,5-Diaryl-1H-pyrazole as a molecular scaffold for the synthesis of apoptosis-inducing agents. *Bioorg. Med. Chem.* **2010**, *18*, 3270−3278.
(55) Padmavathy, K.; Krishnan, K. G.; Kumar, C. U.; Sutha, P.; Sivaramakarthikeyan, R.; Ramalingan, C. Synthesis, Antioxidant Evaluation, Density Functional Theory Study of Dihydropyrimidine Festooned Phenothiazines. *ChemistrySelect* **2018**, *3*, 5965−5974.
(56) Krishnan, K. G.; Ashothai, P.; Padmavathy, K.; Lim, W.-M.; Mai, C.-W.; Thanikachalam, P. V.; Ramalingan, C. Hydrazide-integrated carbazoles: synthesis, computational, anticancer and molecular docking studies. *New J. Chem.* **2019**, *43*, 12069−12077.
(57) Padmavathy, K.; Krishnan, K. G.; Kumar, C. U.; Sathiyaraj, E.; Sivaramakarthikeyan, R.; Lim, W.-M.; Mai, C.-W.; Ramalingan, C. Novel acrylamide/acrylonitrile-tethered carbazoles: synthesis, structural, biological, and density functional theory studies. *New J. Chem.* **2019**, *43*, 13418−13429.
(58) Krishnan, K. G.; Kumar, C. U.; Lim, W.-M.; Mai, C.-W.; Thanikachalam, P. V.; Ramalingan, C. Novel cyanoacetamide integrated phenothiazines: Synthesis, characterization, computational studies and in vitro antioxidant and anticancer evaluations. *J. Mol. Struct.* **2020**, *1199*, 127037.
(59) Mizushima, Y.; Kobayashi, M. Interaction of anti-inflammatory drugs with serum proteins, especially with some biologically active proteins. *J. Pharm. Pharmacol.* **1968**, *20*, 169−173.
(60) Rajesh, M. P.; Natvar, J. P. In vitro antioxidant activity of coumarin compounds by DPPH, Super oxide and nitric oxide free radical scavenging methods. *J. Adv. Pharm. Educ. Res.* **2011**, *1*, 52−68.
(61) Rida, S.; Youssef, A.; Badr, M.; Malki, A.; Sherif, Z.; Sultan, A. Design, synthesis and evaluation of novel benzimidazoles, benzothiazoles and benzofurans incorporating pyrazole moiety as antiangiogenic agents. *Arzneim.-Forsch.* **2012**, *62*, 63−74.
(62) Er, J. L.; Goh, P. N.; Lee, C. Y.; Tan, Y. J.; Hii, L.-W.; Mai, C. W.; Chung, F. F.-L.; Leong, C.-O. Identification of inhibitors synergizing gemcitabine sensitivity in the squamous subtype of pancreatic ductal adenocarcinoma (PDAC). *Apoptosis* **2018**, *23*, 343−355.
(63) Chung, F. F.-L.; Tan, P. F. T. M.; Raja, V. J.; Tan, B.-S.; Lim, K.-H.; Kam, T.-S.; Hii, L.-W.; Tan, S. H.; See, S.-J.; Tan, Y.-F.; Wong, L.-Z.; Yam, W. K.; Mai, C. W.; Bradshaw, T. D.; Leong, C.-O. Jerantinine A induces tumor-specific cell death through modulation of splicing factor 3b subunit 1 (SF3B1). *Sci. Rep.* **2017**, *7*, 42504.
(64) Yeong, K. Y.; Tan, S. C.; Mai, C.-W.; Leong, C.-O.; Chung, F. F.-L.; Lee, Y. K.; Chee, C. F.; Abdul Rahman, N. Contrasting sirtuin and poly(ADP-ribose)polymerase activities of selected 2,4,6-trisubstituted benzimidazoles. *Chem. Biol. Drug Des.* **2018**, *91*, 213−219.
(65) Mai, C.-W.; Kang, Y.-B.; Nadarajah, V. D.; Hamzah, A. S.; Pichika, M. R. Drug-like dietary vanilloids induce anticancer activity through proliferation inhibition and regulation of bcl-related apoptotic proteins. *Phytother. Res.* **2018**, *32*, 1108−1118.
(66) Mai, C. W.; Yap, K. S. I.; Kho, M. T.; Ismail, N. H.; Yusoff, K.; Shaari, K.; Chin, S. Y.; Lim, E. S. H. Mechanisms underlying the anti-inflammatory effects of *clinacanthus nutans* lindau extracts: inhibition of cytokine production and toll-like receptor-4 activation. *Front. Pharmacol.* **2016**, *7*, 7.
(67) Soo, H.-C.; Chung, F. F.-L.; Lim, K.-H.; Yap, V. A.; Bradshaw, T. D.; Hii, L.-W.; Tan, S.-H.; See, S.-J.; Tan, Y.-F.; Leong, C.-O.; Mai, C.-W. Cudraflavone C induces tumor-specific apoptosis in colorectal cancer cells through inhibition of the phosphoinositide 3-kinase (PI3K)-AKT pathway. *PLoS One* **2017**, *12*, e0170551.
(68) Ramalingan, C.; Jayalakshmi, L.; Stalindurai, K.; Karuppasamy, A.; Sivaramakarthikeyan, R.; Devadoss, V. A Green and facile synthesis of bio pertinent pyrazole-decorated nitriles and acrylates under catalyst-free conditions. *Synlett* **2015**, *26*, 1857. , and references cited therein

https://dx.doi.org/10.1021/acsomega.0c00630
ACS Omega 2020, 5, 10089−10098